

The Fluence Distribution of Gamma-Ray Bursts

Vahé Petrosian¹ and Theodore T. Lee²

Center for Space Science and Astrophysics, Stanford University, Stanford, CA 94305-4060

Received _____; accepted _____

arXiv:astro-ph/9606019v1 4 Jun 1996

²Department of Applied Physics

¹Departments of Physics and Applied Physics

ABSTRACT

In the use and interpretation of $\log N$ – $\log S$ distributions for gamma-ray bursts, burst peak flux has typically been used for S . We consider here the use of the fluence as a measure of S , which may be a more appropriate quantity than the peak flux in such highly variable sources. We demonstrate how using the BATSE trigger data we can determine the selection effects on fluence. Then using techniques developed elsewhere to account for the important threshold effects and correlations. Applying the appropriate corrections to the distributions, we obtain a fluence distribution which shows a somewhat sharper break than the peak flux distribution, implying a possibly narrower fluence luminosity distribution. If bursts are at cosmological distances, these observations together indicate that evolution of the luminosity function is required.

Subject headings: gamma rays: bursts

1. Introduction

Because of their transient nature and lack of counterparts, the distance to Gamma-Ray Bursts (GRBs) is not known. Statistical distributions have therefore been used as indirect means of estimating their distances. The original discovery by the Burst and Transient Source Experiment (BATSE) team (Meegan et al. 1992), and the subsequent confirmations (Meegan 1996) that GRBs are isotropically distributed in the sky has gradually strengthened cosmological interpretations of GRB sources. If bursts are indeed of a cosmological origin, then the so-called $\log N$ - $\log S$ distribution can be used to constrain the model parameters.

Under the assumption that bursts are distributed homogeneously and isotropically in a static Euclidean space (HISE), the logarithmic slope of the $\log N$ - $\log S$ distribution is expected to be $-3/2$. In cosmological scenarios, the observed deviations from this slope are due to the breakdown of the last two conditions in HISE. The degree of deviation depends on not only the geometry and expansion rate of space but also the shape and evolution of the luminosity function. This latter effect is less significant for narrow and slowly evolving luminosity functions, but if the range of luminosities is larger than the observed range of S , it will obscure the cosmological effects. Therefore the choice of the parameter S is important in the interpretation of the $\log N$ - $\log S$ results.

For steady sources, this choice is obvious; S would be represented by the steady and well-defined photon or energy flux. However, for highly transient sources such as GRBs, the measured flux depends on the time scale over which the burst is observed. Ideally, one would like the flux measure to be instantaneous, defined such that the observational time scale for the accumulation of photons is smaller than the intrinsic variation time scale of the source. In practice, observational measures such as the “peak flux” have been averaged over a time interval Δt which might not be small compared to the intrinsic time scale. Use of this version of the “peak flux” for the parameter S in the $\log N$ - $\log S$ distributions can

lead to ambiguous interpretations, and a number of complicated steps have to be taken in order to extract the instantaneous peak flux distribution from the data (see Lee & Petrosian 1996a, hereafter LP).

These complications can be avoided by using a different observational measure for S . One such measure is the fluence \mathcal{F} , which we define to be the total (time-integrated) radiant energy per unit area within the BATSE trigger range of 50–300 keV. The fluence distribution may prove to be a more useful tool in cosmological studies than the peak flux distribution if the time-integrated luminosity has a narrower intrinsic dispersion and undergoes less evolution than the peak luminosity. In fact, given the wide dispersion in the durations of GRBs, it is difficult to justify why the intensity of the highest spike in a bursting source should have a narrow distribution. Perhaps the total energy released has a narrower distribution than that of the peak luminosity. For example, it is more likely that the total energy released in a compact object merger might be a more appropriate “standard candle” than the rate of energy release in such a merger. Furthermore, in cosmic fireball models which presumably describe the physics of these mergers, the relationship between the luminosity observed in the detector’s rest frame to that emitted by the source depends strongly on the bulk Lorentz factor of the expanding shell (Meszaros & Rees 1993, 1994; Madras & Fenimore 1996), which is not likely to be universal for all bursts.

In this paper we investigate the $\log N$ - $\log \mathcal{F}$ relation for BATSE GRBs. In the next section we describe how a bias-free fluence distribution can be obtained from instruments such as BATSE which trigger on some average flux value. In §3 we discuss our results.

2. Analysis

2.1. Obtaining the Fluence Limit

We use the publicly available BATSE 3B catalog data, which provides the maximum and minimum photon counts C_{max} and C_{min} for the three trigger time intervals $\Delta t = 64, 256, 1024$ ms. The most fundamental selection effect is that C_{max} must exceed the threshold C_{min} . We are interested in the more physically meaningful fluences and fluxes. The BATSE catalog also gives values of the total energy fluence \mathcal{F} within the 50–300 keV range, along with three measures of the average peak flux. The average peak flux is given by $\bar{f}_P = C_{max}/(A_{eff}(\theta, \phi)\Delta t)$, where A_{eff} is the effective detector area (including the spectral response) of the instrument in the direction (θ, ϕ) .

Given \bar{f}_P or \mathcal{F} , we ask what would have been the threshold for detection of a burst for any of these quantities. It is easy to see that a burst with average peak flux \bar{f}_P coming from a direction θ and ϕ would trigger BATSE if $\bar{f}_P > \bar{f}_{lim} \equiv C_{min}/(A_{eff}(\theta, \phi)\Delta t)$. Otherwise C_{max} would be less than C_{min} . Therefore, the threshold on the average peak flux is $\bar{f}_{lim} = \bar{f}_P C_{min}/C_{max}$. The same relation also exists for the fluence and its limit, as can be seen schematically by examining Figure 1. A burst with observed fluence \mathcal{F} (or \bar{f}_P) and a particular pulse profile, spectrum, etc. would have been undetected if its fluence (or flux) was lowered by a factor of C_{max}/C_{min} , because then its peak counts C_{max} would have been less than the limiting counts C_{min} . Clearly then $\mathcal{F}_{lim} = \mathcal{F} C_{min}/C_{max}$, as long as the background count rate does not vary significantly throughout the duration of the burst. In summary,

$$\frac{C_{max}}{C_{min}} = \frac{\bar{f}_P}{\bar{f}_{lim}} = \frac{\mathcal{F}}{\mathcal{F}_{lim}}. \quad (1)$$

The last equality is approximate because of the implicit conversion between photon counts and energy. This will be a good approximation if the source spectra do not change drastically throughout the duration of the burst.

Note that all of the details of the pulse profile, spectrum, and instrumental response are

hidden in the ratio. The problem of obtaining the distribution of any of the quantities in equation (1) can be described generally as the problem of obtaining the distribution of some variable x subject to the condition that $x_i > x_{i,lim}$ for each data point i . A general solution to this problem was described by Petrosian (1993) and has been extensively discussed in LP. It can be seen that extracting the fluence distribution is in principle no different from extracting the peak flux distribution. It should also be noted that the conclusions drawn from the distribution of V/V_{max} or its average are unchanged no matter which of these properties is used as a measure of distance.

2.2. Fluence Limit Interpretation

Although the extraction of the fluence distribution is computationally straightforward, the interpretation of \mathcal{F}_{lim} differs from that of C_{min} and hence deserves some explanation. C_{min} is simply a threshold that depends only on the background count rate and is a variable independent of the physical burst properties. For bursts which have durations $T \ll \Delta t$ it is clear that $\mathcal{F} = C_{max}\langle h\nu\rangle/A_{eff}(\theta, \phi)$ and $\mathcal{F}_{lim} = C_{min}\langle h\nu\rangle/A_{eff}(\theta, \phi)$ are independent, where $\langle h\nu\rangle$ is the average photon energy in the 50–300 keV range. For long duration bursts with $T > \Delta t$, we have approximately $\mathcal{F} \propto \bar{f}_p T \langle h\nu\rangle$, so that from equation (1) we obtain

$$\mathcal{F}_{lim} = \langle h\nu\rangle T \frac{C_{min}}{A_{eff}(\theta, \phi)\Delta t}, \quad (2)$$

indicating that if as expected $\langle h\nu\rangle$, $A_{eff}(\theta, \phi)$, and C_{min} are essentially independent of \mathcal{F} , the fluence limit is approximately proportional to the duration.

2.3. Fluence Distributions

We now examine all bursts for which a fluence measurement and a value of C_{max}/C_{min} exists. The values of C_{max}/C_{min} are known for three time scales: 64 ms; 256 ms; and

1024 ms. We use the 1024 ms values of C_{max}/C_{min} because this time scale is the most sensitive and allows us to use the largest number of bursts, but we also note that the other time scales give essentially identical results. Note that unlike in the determination of the distribution of instantaneous peak flux (see LP), where a correction for the short duration bias based on some observational duration measure was necessary, there is no need to have a separate measure of duration to determine the fluence limit. This increases the number of bursts available from 514 to 555 for the 1024 ms trigger. It may be argued that bursts with no well-defined durations may have data gaps or some other problems which would make the fluence measurements unreliable. As it turns out, the resulting fluence distributions are insensitive to whether or not we include the extra 41 bursts.

The bivariate distribution of \mathcal{F} and \mathcal{F}_{lim} is shown in the top panel of Figure 2. Obviously because of the data truncation due to the variation in \mathcal{F}_{lim} , simply binning the fluences to get a distribution will result in a biased distribution. As explained by Petrosian (1993), a nonparametric method exists to obtain a single variable distribution from a truncated bivariate distribution. This method amounts to using information from untruncated regions to estimate the data that was missed due to the truncation. Clearly, this is only possible provided the variables are uncorrelated. The first thing we must do is test the data for a correlation between \mathcal{F} and \mathcal{F}_{lim} . Using the correlation test designed for use on truncated data (Efron & Petrosian 1992), we find that the probability that the data are uncorrelated is 2.3×10^{-5} . As discussed in §2.2, since \mathcal{F}_{lim} is approximately proportional to the duration, a correlation test involving \mathcal{F} and \mathcal{F}_{lim} effectively tests the correlation between fluence and duration. The results indicate that the fluence and the duration are positively correlated with each other. If the fluence is a good measure of distance, this result seems to be in the opposite sense of that expected from cosmological time dilation (c.f. Norris 1995). However, there are a number of factors which could complicate this interpretation (see Lee & Petrosian 1996b).

In order to go further, one must resort to parameterizing the correlation. As we have done before (Lee, Petrosian, & McTiernan 1993; 1995; LP), we use a simple power law parameterization. Briefly, we transform \mathcal{F}_{lim} into $\mathcal{F}'_{lim} = \mathcal{F}_{lim}\mathcal{F}^{-\alpha}$ and vary α until the correlation between \mathcal{F} and \mathcal{F}'_{lim} disappears. This requirement gives a well-defined value for α . We find $\alpha = 0.22 \pm 0.07$, with the error interval indicating the $\pm 90\%$ confidence limits on α . The data truncation boundaries are transformed accordingly. The resulting bivariate distribution, which now contains uncorrelated variables, is shown in the bottom panel of Figure 2, which can then be readily integrated over \mathcal{F}'_{lim} with the methods described in LP. Using this technique, we obtain the cumulative and differential distributions of \mathcal{F} , along with the logarithmic slope of the cumulative distribution as a function of \mathcal{F} (Fig. 3). The qualitative shapes of these distributions persist even if we use different samples of bursts corresponding to higher fluence limits. We justify the particular parameterization chosen here (power law) by noting that similar values of α are found for data subsets chosen from various ranges in \mathcal{F} , and in any case the dispersion in the data is such that there would be little justification for a more complicated parameterization.

Dividing our best estimate of the differential distribution $n(\mathcal{F})$ by what would have been obtained without consideration of the truncation and correlation gives the trigger efficiency as a function of fluence, which is plotted in Figure 4 along with the ratio of the observed number of bursts $N_{obs}(> \mathcal{F})$ to the total number of bursts $N(> \mathcal{F})$ greater than a given fluence \mathcal{F} . Our derived efficiency can be compared to the results of in't Zand & Fenimore (1996) and Bloom, Fenimore, & in't Zand (1996), who utilize a quite different approach. Rather than starting with the data and working backwards through the selection effects to derive the distributions, in't Zand & Fenimore use Monte Carlo simulations of a sample of bursts with a distribution of temporal and spectral shapes as observed by BATSE. Then assuming a cosmological origin for the sources, they predict the trigger efficiency of BATSE as a function of fluence. In contrast, our “efficiency” is purely

empirical and involves no model assumptions. Using these trigger efficiencies, Bloom et al. (1996) correct the observed fluence distributions to obtain the true distributions. Their results are qualitatively similar to ours, although their $\log N$ - $\log \mathcal{F}$ curve has a very steep upturn at low fluences which is not evidenced in our curves. This difference may arise as a result of their assumption that any correlations between burst characteristics are solely a result of cosmological effects such as time dilation and redshifting. However, it would be very difficult to reconcile the strong positive correlation that we found between fluence and duration with any non-evolving cosmological population of bursts.

3. Discussion and Conclusions

We have described a robust method of accounting for the selection biases on the detection of BATSE GRBs based on their fluences, independent of duration or spectral measures. Using methods described in our previous publications we have obtained the variation of the cumulative distribution, differential distribution, and logarithmic slope of the distribution as a function of fluence. The results shown in Figure 3 reveal that the fluence distribution appears to show a sharp break from slope $-3/2$ to about $-1/2$ at $\mathcal{F} \approx 10^{-5}$ erg cm $^{-2}$. The analogous peak flux distributions (see Fig. 7 of LP for an example) show a slightly more gradual transition in slope. Our interpretation of this result would be that the time-integrated luminosity has a narrower distribution than the peak luminosity. Therefore the fluence may be a better indicator of the burst distance than the peak flux. The lack of consistency with the time dilation effect would imply that either the burst sources are not cosmological or models more complicated than the simple no-evolution model are necessary.

Ignoring the inconsistency for the moment, fits of the fluence distribution to very simple cosmological models (constant comoving density, no luminosity evolution, energy

spectra either power laws or as in Band et al. (1993), density parameter $\Omega = 0$ or 1, $H_0 = 75 \text{ km s}^{-1} \text{ Mpc}^{-1}$) give sources of total radiant energy $\mathcal{E} \sim 10^{52}$ ergs or $\mathcal{E} \sim 10^{51}$ ergs for $\Omega = 0$ and $\Omega = 1$ models, respectively. Note that uncertainties in the spectral form can be absorbed into uncertainties in the luminosity evolution, and in any case the data are not sensitive enough to definitively distinguish among the models. A difference between these models and those involving peak fluxes is that the inferred maximum redshifts are greater ($z_{max} \approx 3$ for the models involving power law spectra and $z_{max} \approx 5$ for the models utilizing the Band spectral form), a result also noted by Bloom et al. (1996). However, adding in the evolution necessary for agreement with the time dilation results would reduce these inferred maximum redshifts.

We acknowledge W. Azzam and G. Pendleton for useful discussions, and we thank the anonymous referee for comments and suggestions which led to an improved paper. This work was funded by NASA grants NAGW 2290 and NAG-5 2733.

REFERENCES

- Band, D. et al. 1993, ApJ, 413, 281
- Bloom, J. S., Fenimore, E. E., & in't Zand, J. 1996, proceedings of the 3rd Huntsville Gamma-Ray Burst Symposium, in press
- Efron, B. & Petrosian, V. 1992, ApJ, 399, 345
- Lee, T. T. & Petrosian, V. 1996a, ApJ, in press (LP)
- Lee, T. T., & Petrosian, V., 1996b, ApJ, in preparation
- Lee, T. T., Petrosian, V., & McTiernan, J. M. 1993, ApJ, 412, 401
- Lee, T. T., Petrosian, V., & McTiernan, J. M. 1995, ApJ, 448, 915
- in't Zand, J. J. M., & Fenimore, E. E. 1996, proceedings of the 3rd Huntsville Gamma-Ray Burst Symposium, in press
- Madras, C. D., & Fenimore, E. E. 1996, proceedings of the 3rd Huntsville Gamma-Ray Burst Symposium, in press
- Meegan, C. A., Fishman, G. J., Wilson, R. B., Paciesas, W. S., Pendleton, G. N., Horack, J. M., Brock, M. N., & Kouveliotou, C. 1992, Nature, 355, 143
- Meszaros, P. & Rees, M. J. 1993, ApJ, 405, 278
- Meszaros, P. & Rees, M. J. 1994, ApJ, 430, L93
- Norris, J. P., Bonnell, J. T., Nemiroff, R. J., Scargle, J. D., Kouveliotou, C., Paciesas, W. S., Meegan, C. A., & Fishman, G. J. 1995, ApJ, 439, 542
- Petrosian, V. 1993, ApJ, 401, L33

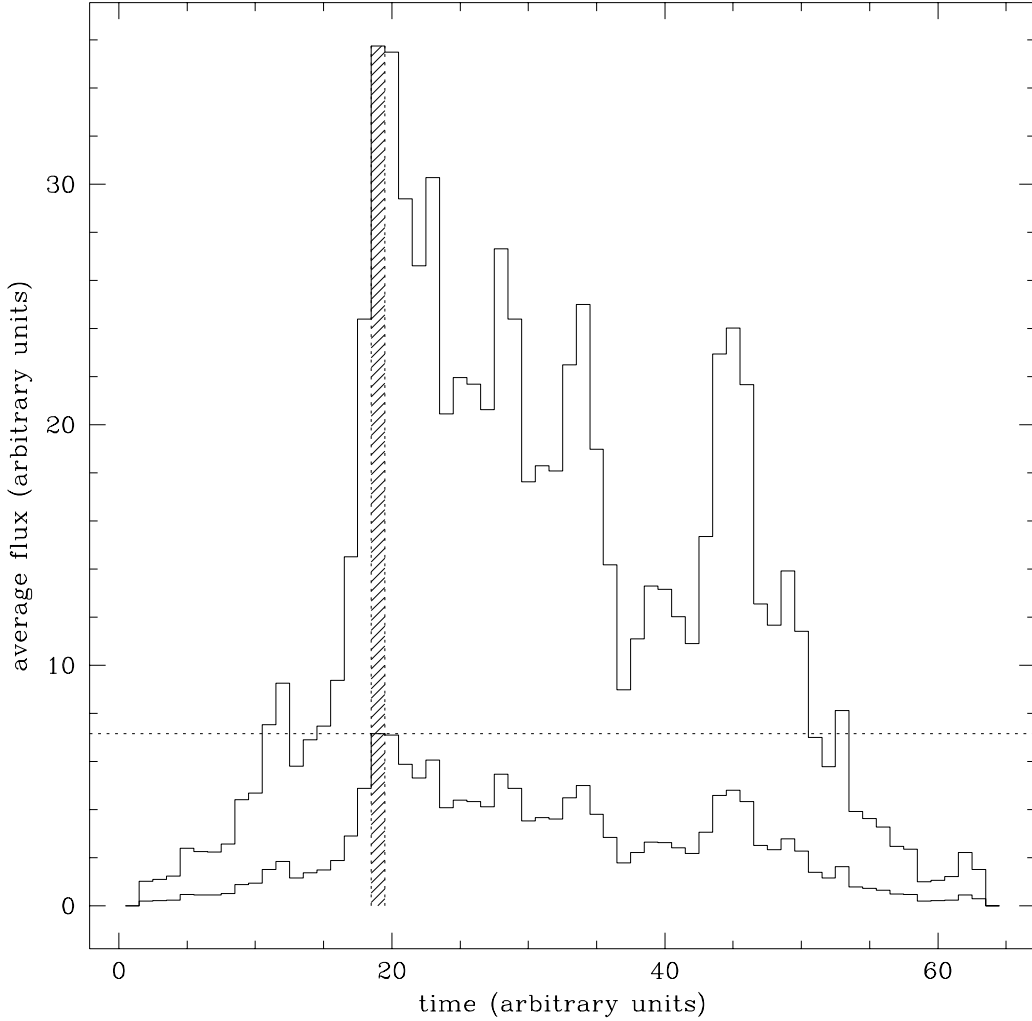


Fig. 1.— Schematic diagram of burst selection. The larger histogram represents the light curve of a typical burst. Neglecting spectral variation effects, the fluence is proportional to the time integral of the curve. The shaded bin represents the peak flux of the burst (integrated over the trigger time), and the dotted line represents the average value of the limiting flux, below which the burst would not have triggered. The smaller histogram shows the light curve scaled down by a factor of \bar{f}_P/\bar{f}_{lim} (or equivalently C_{max}/C_{min}). No matter what the light curve looks like, it can be seen that if C_{max}/C_{min} is constant throughout the burst, then the limiting fluence for the burst is simply given by the fluence scaled by C_{max}/C_{min} .

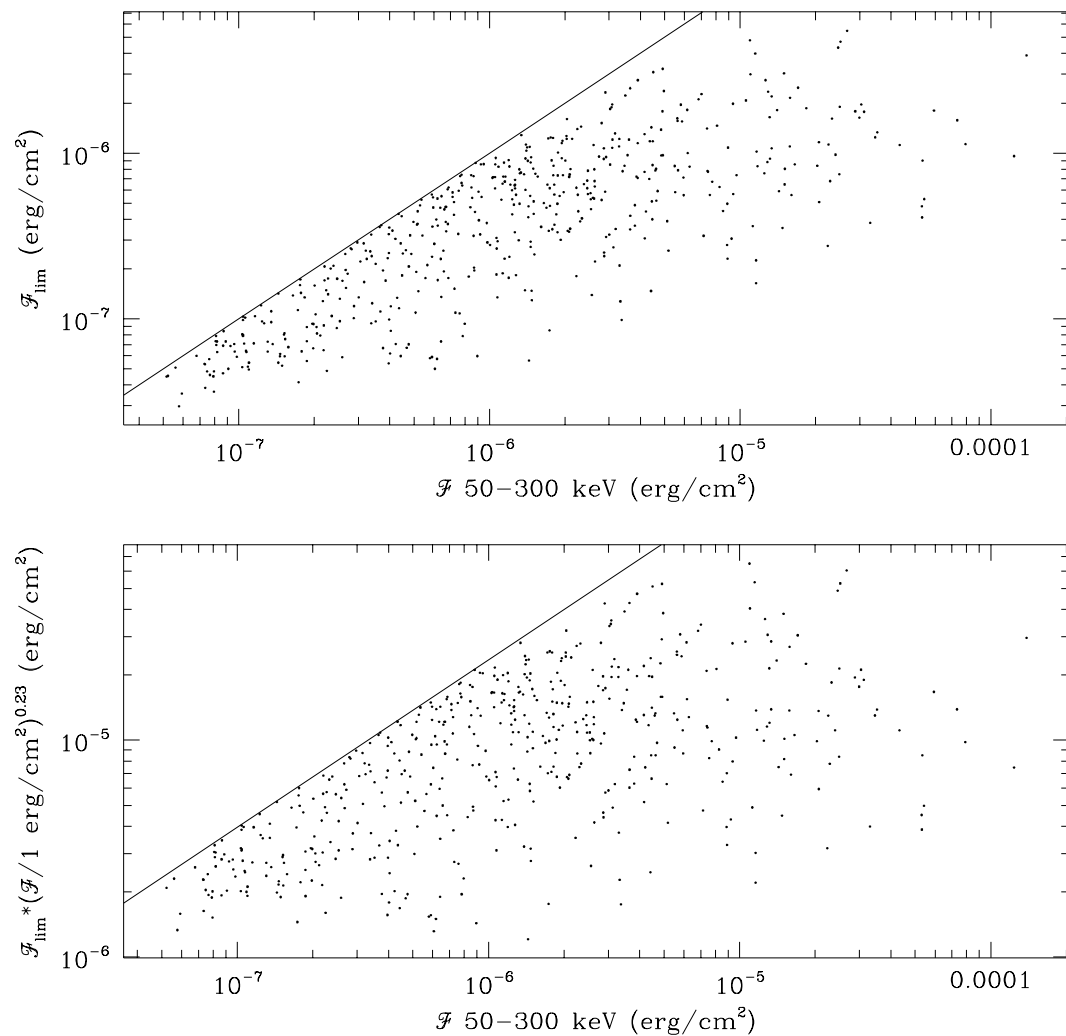


Fig. 2.— *top panel*: Bivariate distribution of \mathcal{F} and \mathcal{F}_{lim} . The diagonal line indicates the selection criterion $\mathcal{F} > \mathcal{F}_{lim}$. *bottom panel*: Bivariate distribution of \mathcal{F} and $\mathcal{F}'_{lim} = \mathcal{F}_{lim}\mathcal{F}^{-\alpha}$, with $\alpha = 0.23$. The diagonal line indicates the selection criterion $\mathcal{F} > \mathcal{F}'_{lim}$.

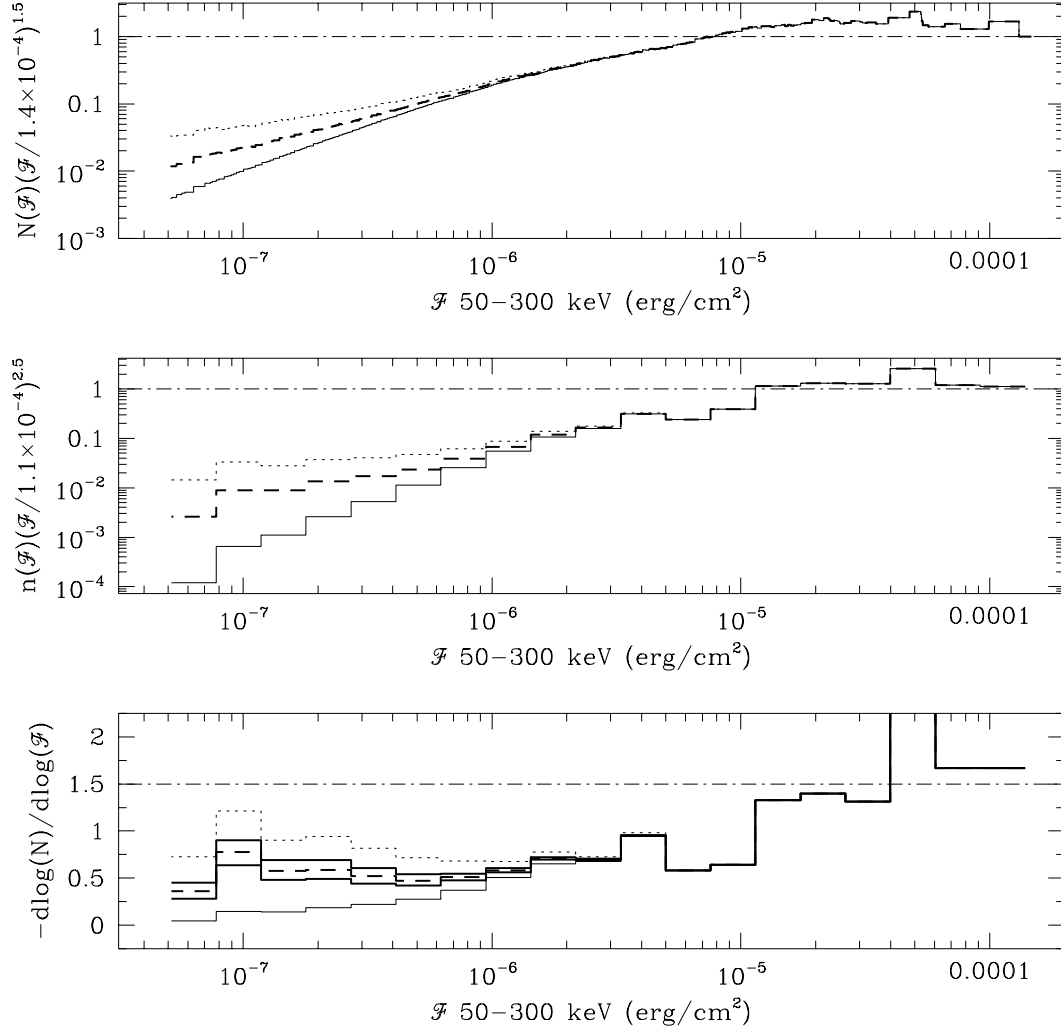


Fig. 3.— *top panel:* Cumulative distribution $N(\mathcal{F})\mathcal{F}^{1.5}$ of fluence, showing the deviation from HISE. The solid histogram is the distribution that would have been obtained without consideration of selection effects or correlations. The dotted histogram is the distribution that would have been obtained by accounting for selection effects but neglecting correlation. The solid histogram is the distribution obtained when accounting for both effects. The dot-dashed line indicates the HISE prediction of logarithmic slope -1.5. *middle panel:* The differential distribution multiplied by $\mathcal{F}^{5/2}$, which shows the deviation from the HISE prediction (dot-dashed line). *bottom panel:* Logarithmic slope of N as a function of \mathcal{F} . The heavy solid lines show the 90% confidence limits on the transformation used to remove the correlation.

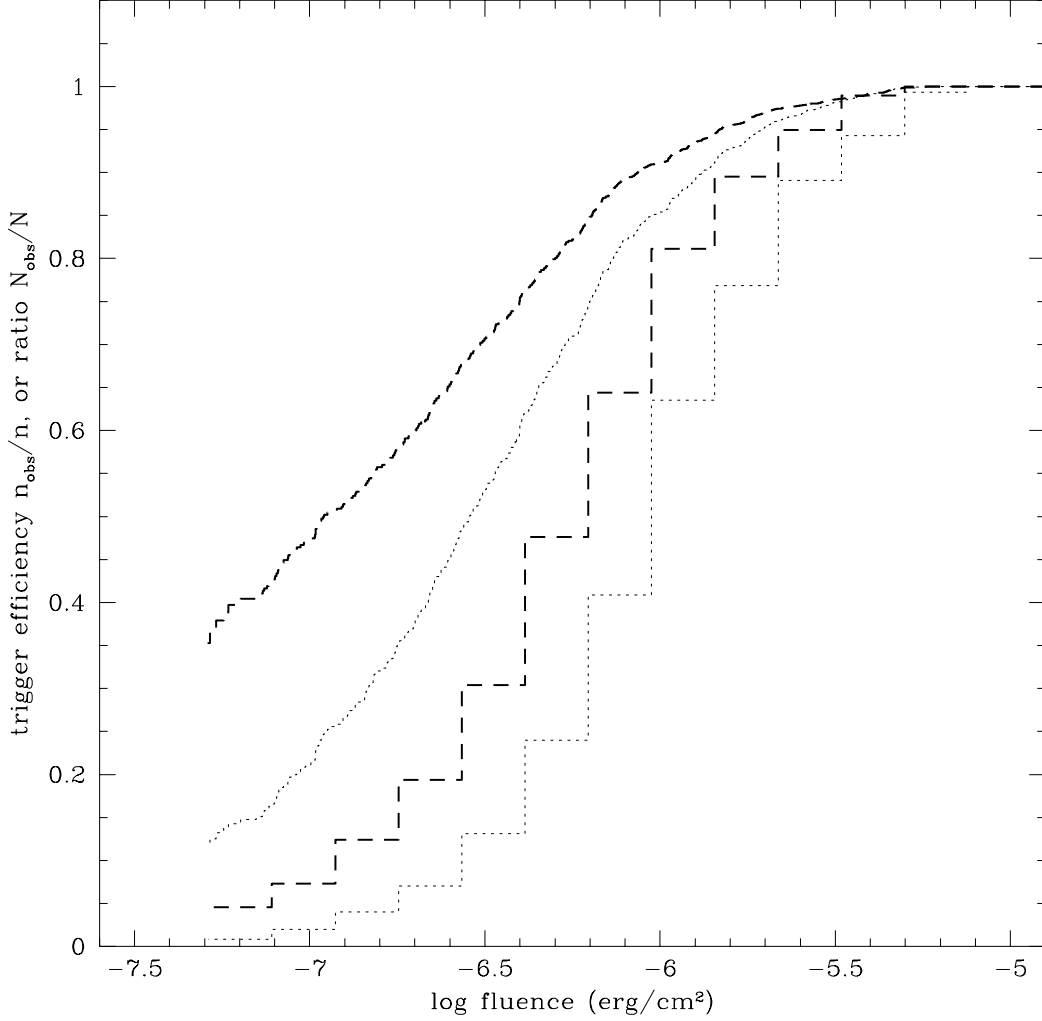


Fig. 4.— The lower two histograms show the trigger efficiency $n_{obs}(\mathcal{F})/n(\mathcal{F})$ as a function of fluence, while the upper two histograms show the ratio of the cumulative number of bursts observed $N_{obs}(> \mathcal{F})$ to the true cumulative number of bursts $N(> \mathcal{F})$. The dashed lines depict our best estimates of the trigger efficiency and ratio of observed to total number of bursts, accounting for both data truncation and correlation. The dotted lines depict the efficiency or ratio without accounting for the effects of correlation.